

# Strained Layer Crystalline Undulator

A. Kostyuk

Ostmarkstraße 7, 93176 Beratzhausen, Germany

---

## Abstract

Ultrarelativistic charged particles are predicted to emit hard electromagnetic radiation of undulator type while being channeled in a crystal with periodically bent crystallographic planes. The recently proposed crystalline undulator with the bending amplitude smaller than the distance between the bent planes and the bending period shorter than the period of channeling oscillations is far superior to what was proposed previously. In the same time, it is more challenging from the technical point of view because its bending period has to be in the sub-micron range. It is shown that a mixed crystal of silicon-germanium with properly varying germanium fraction can have the necessary bending parameters. Moreover, it is predicted to be stable against misfit dislocations.

*Keywords:* strained layer superlattice, crystalline undulator

*PACS:* 68.65.Cd, 46.25.Cc, 61.72.uf, 61.85.+p

---

Channeling [1, 2] of ultrarelativistic charged particles through a periodically bent crystal can be used to generate hard electromagnetic radiation of undulator type [3, 4]. Such a radiation source may become a compact and affordable alternative to presently existing synchrotron radiation sources that are widely used in science and technology [5] but are very big and expensive. Moreover, a coherent radiation source, a hard X ray or gamma ray laser, can be built on the basis of the crystalline undulator [6].

Initially, it was suggested that the charged projectiles should follow the sinusoidal shape of the bent crystallographic planes of the crystalline undulator performing nearly harmonic transverse oscillations. Due to these oscillations, the spectrum of the electromagnetic radiation emitted by the particles in the forward direction was expected to have a narrow peak, similarly as it took place in an ordinary (magnetic) undulator [7, 8, 9].

Several conditions had to be satisfied by the crystal and the beam to reach the desirable properties of the spectrum [10]. In particular, the bending period had to be much larger than the period of channeling oscillations,  $\lambda_u \gg \lambda_c$ . Otherwise the projectile would not follow the shape of the bent crystal channel. Additionally, the bending amplitude should be much larger than the distance between the guiding crystallographic planes,  $a_u \gg d$ , to make sure that the spectrum is dominated by the undulator peak rather than by the channeling radiation, which is present also in the case of a straight crystal [11]. In the following, such a crystalline undulator will be referred to as LALP CU (**l**arge **a**mplitude and **l**ong **p**eriod **c**rystalline **u**ndulator).

A new type of crystalline undulator has been proposed recently [12] (see also [13]). It has been demonstrated by numerical simulations that a crystalline undulator with a bending

period smaller than the channeling period,

$$\lambda_u < \lambda_c \quad (1)$$

and the bending amplitude smaller than the channel width

$$a_u < d \quad (2)$$

has certain advantages over LALP CU. In particular, it has a much larger effective number of undulator periods and it requires much lower beam energy for the production of radiation of a given frequency comparing to LALP CU. The new type of crystalline undulators is referred to as SASP CU (**s**mall **a**mplitude and **s**hort **p**eriod **c**rystalline **u**ndulator).

Channeling of electrons and positrons in SASP CU has been simulated with the computer code ChaS (**C**hanneling **S**imulator) and the corresponding radiation spectra have been calculated [12]. A comparison to a spectrum of LALP CU has been presented in [13]. In contrast to LALP CU, the channeled projectile in the SASP CU does not follow the shape of the bent planes. Still, the shape of the trajectory does contain a Fourier component with the period equal to that of the undulator bending. As the result, a narrow undulator peak is present in the radiation spectrum of SASP CU. This result has been confirmed by independent computations [14] and verified experimentally [15]. Application of SASP CU to nuclear waste transmutation has been discussed in [16].

The intensity of the radiation is proportional to the fourth power of the frequency. The frequency of the undulator radiation is higher than that of the channeling radiation. Therefore, the intensity of the undulator radiation peak is higher than the channeling one despite of the smallness of the undulator amplitude with respect to the channel width (see [12] and [13] for details).

From technological point of view, SASP CU is more challenging than LALP CU. For moderate projectile energy  $E \lesssim 1$

---

*Email address:* andriy.p.kostyuk@gmail.com (A. Kostyuk)

GeV, it is necessary to bend the crystal with a period shorter than one micron. The purpose of the present letter is to analyze whether the manufacturing of such crystals is possible within presently existing technologies.

Several techniques have been proposed to produce LALP CU. At the very beginning [3, 4], it was suggested to use ultrasonic waves to bend the crystal. However this idea appeared to be too challenging from the technical point of view and, therefore, it is still waiting for its experimental implementation. The attenuation of the acoustic wave is inversely proportional to its wavelength. i.e. the shorter the undulator period, the stronger is the attenuation. Therefore, using ultrasound in the case of the SASP CU would be even more difficult or even impossible.

A few other technologies utilize the idea of imposing periodic stresses on the surface of the crystal sample. It can be accomplished by making regularly spaced grooves on the crystal surface either by a diamond blade [17, 18, 19] or by means of laser-ablation [20].

Alternatively, the periodic stress can be imposed by depositing strips of a different material on the surface of the crystal. It was initially proposed to use crystalline materials with similar but slightly different lattice constants [21]. Later, it was found more practical to depose  $\text{Si}_3\text{N}_4$  layers onto the surface of a silicon crystal [18]. Deposition takes place at high temperature. The stress appears after cooling the crystal to the room temperature due to different coefficients of thermal expansion of the crystal and the deposited material.

Recently, inducing a sub-surface stress of a silicon crystal by implantation of  $\text{He}^+$  ions has been studied [22].

Manufacturing a SASP CU with the surface stress technology is hardly possible for the following reasons. First, the strain that is produced by the surface stress decreases fast with the distance from the surface. Therefore, the crystal dimension in one of the two transverse directions has to be of the order of the undulator period  $\lambda_u$  [23], which is in the sub-micron range for moderate beam energies  $E \lesssim 1$  GeV due to (1). Preparing such a thin crystal and depositing sub-micron sized strips on its surface, not to mention making regularly spaced grooves, are highly problematic. Second, the bending amplitude varies strongly across the crystal. Only the most central part of it having the width of  $\sim \lambda_u/(2\pi)$  has nearly constant bending amplitude [23]. Only this part should be exposed to the beam. This means that the size of the beam spot in the corresponding transverse direction has to be in the range of tens of nanometers and the crystal has to be placed with the corresponding accuracy. Moreover, as in any other channeling experiment, the beam divergence at the entrance to the crystal should not exceed the critical (Lindhard's) angle, which is typically in the range of a few hundreds microradians or smaller. Therefore, the transverse emittance of the beam should not exceed several nm-mrad. None of the existing electron or positron accelerators has such high beam quality [24].

Fortunately, there is one more method of crystal bending which is free from the above flaws. Growing crystals with varying chemical composition [25] creates strain inside the crystal volume rather than on its surface. Therefore, there is no such severe restrictions on the crystal size as in the previous case.

The bending amplitude does not vary across the crystal. Hence the size of the beam spot can be in the range of hundreds of microns or even a few millimeters in both transverse directions. This allows for using beams of moderate quality from presently available accelerators.

The most mature of such technologies is using the method of molecular beam epitaxy for growing  $\text{Si}_{1-\chi}\text{Ge}_\chi$  crystals with periodically varying germanium fraction  $\chi$ . Such heterostructures were intensively studied for the purposes of the semiconductor industry. There is rather extensive practical experience of creating  $\text{Si}_{1-\chi}\text{Ge}_\chi$  strained layer of various thickness from 10 Å to microns or even tens or hundreds of microns. Their properties are rather well known (see, for instance, [26, 27, 28] and references therein). Deflection of the beam by  $\text{Si}_{1-\chi}\text{Ge}_\chi$  strained layer crystals has been studied experimentally, see e.g. [29, 30]. A  $\text{Si}_{1-\chi}\text{Ge}_\chi$  LALP CU is being used in ongoing experiments at Mainz Microtron [31, 32, 33]. Therefore, the further discussion will be focused on this crystalline material. The idea of [25] will be studied in greater details in order to show that it can be used to produce a SASP CU.

Let us consider a  $\text{Si}_{1-\chi}\text{Ge}_\chi$  single crystal that was grown in the direction [001] with varying germanium content  $\chi$ , see Fig. 1. The coordinate axes  $\xi$ ,  $\eta$  and  $\zeta$  are chosen to coincide with the crystallographic axes [100], [010] and [001], respectively. This means that the germanium fraction  $\chi$  depends on  $\zeta$  but does not depend on  $\xi$  and  $\eta$ .

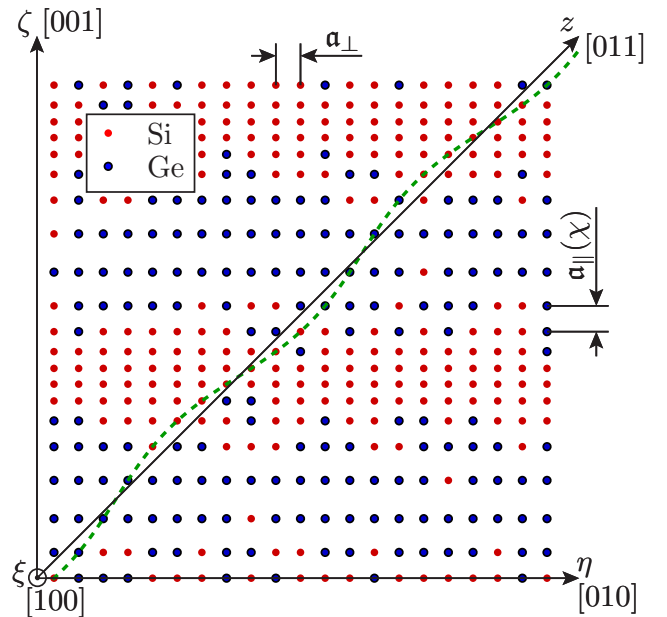


Figure 1: A strained layers superlattice of gradually varying chemical composition. A higher fraction  $\chi$  of germanium results in a larger longitudinal lattice constant  $a_{\parallel}(\chi)$ . Due to the periodic variation of  $\chi$ , the crystal axis [011] (the dashed line) is periodically bent. So is the plane (011), which is perpendicular to the plane of the image and contains the axis [011]. For illustration purposes, the variation of the lattice constant is strongly exaggerated, while the bending period is shown much shorter than it should be in the reality. To simplify the image, only one atom per cubic cell is shown.

Let us take an element of the crystal volume containing  $N$  layers of elementary cells in each direction. The volume has

to be large enough  $N \gg 1$  so that the elasticity theory can be applied. On the other hand, it should not be too large so that the variation of Germanium concentration  $\chi$  could be neglected within the volume element.

Being relaxed, the volume would have a cubic shape with the edge length  $N a(\chi)$  (see Fig. 2). The 'native' lattice constant at given  $\chi$ ,  $a(\chi)$ , can be found from a linear interpolation (Vegard's law [34])<sup>1</sup> between the lattice constants of pure silicon  $a_{\text{Si}}$  and germanium  $a_{\text{Ge}}$ :

$$a(\chi) = (1 - \chi)a_{\text{Si}} + \chi a_{\text{Ge}}. \quad (3)$$

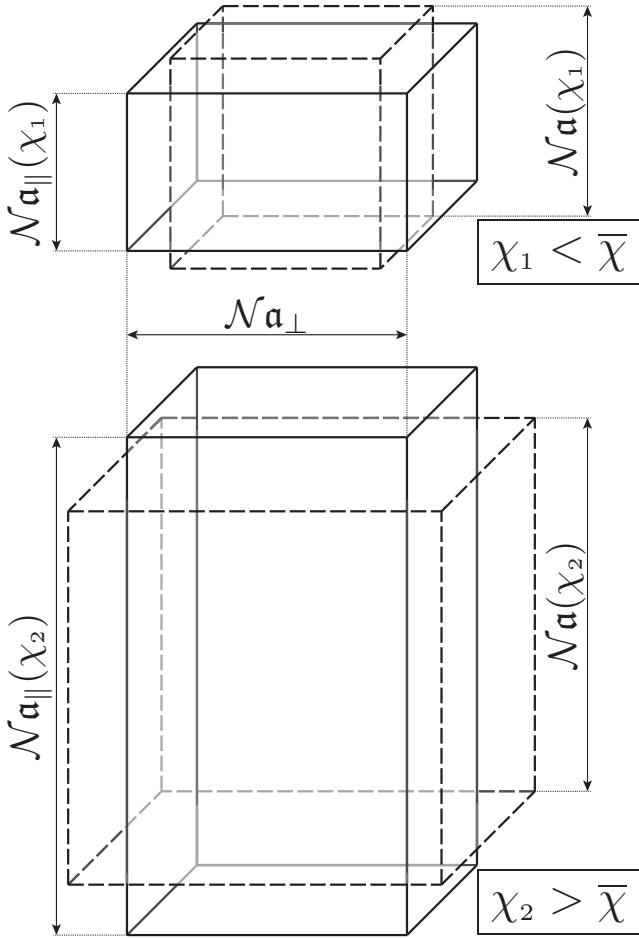


Figure 2: Two pieces of a  $\text{Si}_{1-\chi}\text{Ge}_\chi$  crystal having  $N$  layers of elementary crystal cells in each direction. Being relaxed, each piece would have a cubic shape (shown by dashed lines). Due to different concentrations of germanium,  $\chi_1$  and  $\chi_2$ , the sizes of the cubes,  $N a(\chi_1)$  and  $N a(\chi_2)$ , would be different. In a single crystal, both pieces are forced to have the same transverse size  $N a_\perp$ . Therefore, they are deformed as shown by solid lines. The transverse deformation induces a longitudinal one. The piece with the smaller than average germanium fraction  $\chi_1$  is stretched in the transverse directions,  $a_\perp > a(\chi_1)$ , and contracted in the longitudinal direction,  $a_\parallel(\chi_1) < a(\chi_1)$ . In contrast, the piece with the larger than average germanium fraction  $\chi_2$  is squeezed in the transverse directions,  $a_\perp < a(\chi_2)$ , and elongated in the longitudinal direction  $a_\parallel(\chi_2) > a(\chi_2)$ . For illustration purposes, the deformation of the crystal pieces is exaggerated.

<sup>1</sup>A small deviation [35] from Vegard's law is neglected in the present analysis.

If no defects are present in the crystal, the transverse positions  $(\xi, \eta)$  of the atoms in each crystal layer have to coincide with those of other layers containing different fraction of germanium. For this reason, the actual transverse dimension of the volume element  $N a_\perp$  is, generally speaking, different from  $N a(\chi)$  and does not depend on  $\chi$ . Therefore, the volume element is deformed.

The transverse deformation induces a longitudinal one. Hence, the longitudinal size of the volume element,  $N a_\parallel(\chi)$ , is also, generally speaking, different from  $N a(\chi)$  (see Fig. 2). In contrast to  $a_\perp$ , the longitudinal size of the volume element does depend on  $\chi$ .

The diagonal elements of the strain tensor describing the deformation are

$$\epsilon_{\xi\xi} = \epsilon_{\eta\eta} = \frac{a_\perp - a(\chi)}{a(\chi)}, \quad (4)$$

$$\epsilon_{\zeta\zeta} = \frac{a_\parallel(\chi) - a(\chi)}{a(\chi)} \quad (5)$$

No shear deformation is present.<sup>2</sup> Therefore non-diagonal elements of the strain tensor are zero.

Only three elements of the stiffness tensor  $c$  are independent in the case of crystals with the cubic symmetry (see e.g. [36]). Only two of them,  $C_{11} = c_{\xi\xi\xi\xi} = c_{\eta\eta\eta\eta} = c_{\zeta\zeta\zeta\zeta}$  and  $C_{12} = c_{\xi\xi\eta\eta} = c_{\xi\xi\zeta\zeta} = c_{\eta\eta\xi\xi} = c_{\eta\eta\zeta\zeta} = c_{\zeta\zeta\xi\xi} = c_{\zeta\zeta\eta\eta}$  are relevant to the present analysis. Hence, Hook's law for the deformation (4) and (5) has the following form

$$\sigma_{\xi\xi} = \sigma_{\eta\eta} = (C_{11}(\chi) + C_{12}(\chi)) \frac{a_\perp - a(\chi)}{a(\chi)} + C_{12}(\chi) \frac{a_\parallel(\chi) - a(\chi)}{a(\chi)}, \quad (6)$$

$$\sigma_{\zeta\zeta} = 2C_{12}(\chi) \frac{a_\perp - a(\chi)}{a(\chi)} + C_{11}(\chi) \frac{a_\parallel(\chi) - a(\chi)}{a(\chi)}. \quad (7)$$

The stress tensor  $\sigma$  has to satisfy the following conditions to ensure the mechanical equilibrium of the crystal

$$\overline{\sigma_{\xi\xi}} = \overline{\sigma_{\eta\eta}} = 0 \quad (8)$$

$$\sigma_{\zeta\zeta} = 0. \quad (9)$$

The overline stands for averaging over  $\zeta$ , e.g.

$$\overline{\sigma_{\xi\xi}} = \frac{1}{L_{[001]}} \int_0^{L_{[001]}} \sigma_{\xi\xi} d\zeta. \quad (10)$$

Here  $L_{[001]}$  is the crystal dimension along the crystallographic axis [001].

The elements of stiffness matrix,  $C_{11}(\chi)$  and  $C_{12}(\chi)$ , depend on the germanium concentration  $\chi$ . Because the mechanical

<sup>2</sup>In fact, shear deformation is present at the edges of (001) planes of the crystal, but it decreases fast with the distance from the edge. It is assumed that the sample is sufficiently large in the directions  $\xi$  and  $\eta$  so that the shear deformation can be safely neglected in the bulk of the crystal.

properties of silicon and germanium are rather similar, this dependence can be neglected. The average values  $\overline{C_{11}}$  and  $\overline{C_{12}}$  will be used in the following.

From (7) and (9) one obtains

$$a_{\parallel}(\chi) = a(\chi) - 2 \frac{\overline{C_{12}}}{\overline{C_{11}}} (a_{\perp} - a(\chi)) \quad (11)$$

Substituting the last expression into (7) and (9) yields

$$\left( \frac{a_{\perp} - a(\chi)}{a(\chi)} \right) = 0. \quad (12)$$

The mismatch between the lattice constants of silicon and germanium is small as well. Therefore, the variation of  $a(\chi)$  in the denominator can be also neglected. Hence, one obtains from (12) and (3)

$$a_{\perp} = \bar{a} = (1 - \bar{\chi})a_{\text{Si}} + \bar{\chi}a_{\text{Ge}}. \quad (13)$$

Substituting the last expression into (11) one obtains

$$a_{\parallel}(\chi) = \bar{a} + \tilde{\chi} \left( 1 + 2 \frac{\overline{C_{12}}}{\overline{C_{11}}} \right) \Delta \quad (14)$$

with

$$\tilde{\chi} = \chi - \bar{\chi} \quad (15)$$

and

$$\Delta = a_{\text{Ge}} - a_{\text{Si}}. \quad (16)$$

The angle  $\delta$  between the axes [010] and [011] (cf. Fig. 3) satisfies the following equality

$$\tan \delta = \frac{a_{\parallel}(\chi)}{a_{\perp}} = 1 + \tilde{\chi} \left( 1 + 2 \frac{\overline{C_{12}}}{\overline{C_{11}}} \right) \frac{\Delta}{\bar{a}}. \quad (17)$$

Let us direct the coordinate axis  $z$  along the average direction of the bent crystallographic axis [011], as it is shown in Fig. 3. The axis  $z$  makes the angle  $\pi/4$  with the axis  $\eta$ . Therefore, the angle between the axis  $z$  and the bent crystallographic axis [011] is

$$\tilde{\delta} = \delta - \pi/4. \quad (18)$$

Substituting the last expression into (17) and neglecting the terms of the order of  $\tilde{\delta}^2$  or higher yield

$$\tilde{\delta} = \tilde{\chi} \left( \frac{1}{2} + \frac{\overline{C_{12}}}{\overline{C_{11}}} \right) \frac{\Delta}{\bar{a}}. \quad (19)$$

Let the function  $y(z)$  describe the shape of the crystallographic axis [011]. Then

$$\frac{dy}{dz} = -\tan \tilde{\delta} \approx -\tilde{\delta}. \quad (20)$$

Therefore,

$$y(z) = y(0) - \left( \frac{1}{2} + \frac{\overline{C_{12}}}{\overline{C_{11}}} \right) \frac{\Delta}{\bar{a}} \int_0^z \tilde{\chi}(z) dz. \quad (21)$$

In particular, if  $\chi$  varies harmonically with the amplitude  $\tilde{\chi}_0$ ,

$$\chi(z) = \bar{\chi} + \tilde{\chi}(z) = \bar{\chi} + \tilde{\chi}_0 \sin \left( 2\pi \frac{z}{\lambda_u} \right), \quad (22)$$

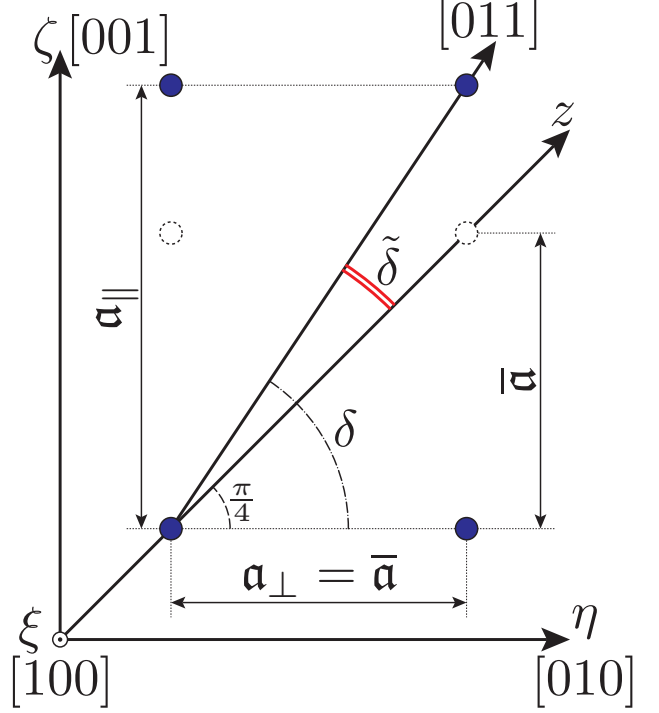


Figure 3: The illustration to the definition of the angles  $\delta$  and  $\tilde{\delta}$ . Due to varying germanium concentration, the size  $a_{\parallel}$  of the crystal cell along the axis  $\zeta$  is, in general case, different from its average value  $\bar{a}$ . Therefore, the angle  $\delta$  between the crystallographic axes [010] and [011] varies around its average value  $\pi/4$ . The angle between the axis [011] and its average direction  $z$  is  $\tilde{\delta}$  (18).

the shape of the bent axis is also harmonic:

$$y(z) = y(0) + a_u \cos \left( 2\pi \frac{z}{\lambda_u} \right), \quad (23)$$

with the bending amplitude

$$a_u = \left( \frac{1}{2} + \frac{\overline{C_{12}}}{\overline{C_{11}}} \right) \frac{\Delta}{\bar{a}} \frac{\lambda_u}{2\pi} \tilde{\chi}_0. \quad (24)$$

Let us rewrite the last expression in the following form<sup>3</sup>

$$\tilde{\chi}_0 = 2\pi \frac{\bar{a}}{\Delta} \left( \frac{1}{2} + \frac{\overline{C_{12}}}{\overline{C_{11}}} \right)^{-1} \frac{a_u}{\lambda_u}. \quad (25)$$

The average quantities in the right hand side depend on  $\bar{\chi}$ .

Let us first consider a small-amplitude variation of  $\chi(z)$  between 0 (pure silicon) and  $2\tilde{\chi}_0$ :

$$\bar{\chi} = \tilde{\chi}_0 \ll 1. \quad (26)$$

In this case,  $\bar{\chi} = 0$  can be substituted into the right hand side of equation (25), i.e. the parameters of pure silicon can be used instead of the average quantities.

<sup>3</sup>The term  $\overline{C_{12}/C_{11}}$  in the parentheses of Eq.(25) appeared due to the longitudinal deformation that is induced by the transverse one (see Fig. 2 and the two paragraphs after Eq. (3)). The induced deformation was not taken into account in [37]. It was assumed there that  $a_{\parallel}(\chi) = a(\chi)$ . For this reason, the necessary germanium content was overestimated by a factor of about 1.8.

Table 1: Parameters of silicon and germanium: the lattice constant  $a$  and stiffness coefficients  $C_{11}$  and  $C_{12}$  [35, 38, 39].

	$a$ (Å)	$C_{11}$ (GPa)	$C_{12}$ (GPa)
Si	5.431	165.6	63.9
Ge	5.658	126.0	44.0

Using the numerical values from Table 1 one obtains

$$\tilde{\chi}_0 = 170 \frac{a_u}{\lambda_u}. \quad (27)$$

The opposite limit,

$$1 - \bar{\chi} = \tilde{\chi}_0 \ll 1, \quad (28)$$

corresponds to a small-amplitude variation of  $\chi(z)$  between  $1 - 2\tilde{\chi}_0$  and 1 (pure germanium). Substituting the parameters from the last line of Table 1 into (25) yields

$$\tilde{\chi}_0 = 184 \frac{a_u}{\lambda_u}. \quad (29)$$

Interpolating linearly between two extreme cases (27) and (29) one obtains the formula

$$\tilde{\chi}_0 = [170(1 - \bar{\chi}) + 184\bar{\chi}] \frac{a_u}{\lambda_u}. \quad (30)$$

that is valid for any  $\bar{\chi}$ ,  $0 \leq \bar{\chi} \leq 1$ .

The bending period  $\lambda_u$  and the amplitude  $a_u$  refer to the axial channel [011]. They also valid for the bent planar channel (01 $\bar{1}$ ), provided that the beam is directed into this channel at a small angle to the axis [011].

It should be stressed that the period of the variation of  $\chi$  along the direction of crystal growth [001] is smaller than  $\lambda_u$ :

$$\lambda_{[001]} = \frac{\lambda_u}{\sqrt{2}}. \quad (31)$$

Therefore,

$$\chi(\zeta) = \bar{\chi} - \tilde{\chi}_0 \sin\left(2\pi \sqrt{2} \frac{\zeta}{\lambda_u}\right). \quad (32)$$

Formulas (30) and (32) contain all the necessary information for calculation of the parameters that are needed for manufacturing a strained layer crystalline undulator with desired  $\lambda_u$  and  $a_u$ .

Still, the amplitude  $a_u$  cannot be arbitrary large. There is a maximum theoretically possible value  $a_{th}$  of  $a_u$  at given  $\lambda_u$ . The theoretical limit is set by  $\tilde{\chi}_0 = 0.5$  which is the maximum possible value of  $\tilde{\chi}_0$  corresponding to  $\chi$  varying between 0 and 1. Substituting  $\tilde{\chi}_0 = \bar{\chi} = 0.5$  into (30), one obtains

$$a_{th} = 2.82 \cdot 10^{-3} \lambda_u. \quad (33)$$

However, the theoretical limit usually cannot be reached in practice. It is well known that there exist a critical thickness  $h_c$  of a strained crystal layer in crystalline heterostructures. If

the layer thickness exceeds  $h_c$ , dislocations appear in the crystal lattice that relax the strain.

Let us first consider a strained  $\text{Si}_{1-\chi}\text{Ge}_\chi$  layer grown on a pure silicon substrate. The larger the germanium fraction in the layer, the smaller its critical thickness. To put it differently, there exists a critical value of  $\chi$  for a given layer thickness  $h$  such that the layer of thickness  $h$  is relaxed with dislocations if its germanium fraction  $\chi$  is larger than critical.

The critical layer thickness for stable crystalline heterostructures were studied in [40, 41, 42]. The obtained results differ only slightly. The formula based on the approach of J. W. Matthews and A. E. Blakeslee [41] will be used in the present analysis. The critical germanium fraction for a stable  $\text{Si}_{1-\chi}\text{Ge}_\chi$  layer of thickness  $h$  grown on a pure silicon substrate is [43]

$$\chi_s = \frac{5.5 \text{ \AA}}{h} \ln \frac{h}{1 \text{ \AA}} \quad (34)$$

(the subscript ‘s’ stands for ‘stable’).

To apply formula (34) to the crystalline undulator, the following two points have to be taken into accounts. First, the transverse lattice constant of the crystalline undulator is not equal to that of the pure silicon. It corresponds to the average germanium fraction  $\bar{\chi}$ . Therefore the deviation  $\tilde{\chi}$  from the average concentration has to be compared to  $\chi_s$  instead of  $\chi$ . Second, formula (34) assumes a constant germanium concentration in the epitaxial layer, while  $\tilde{\chi}$  varies between 0 and  $\tilde{\chi}_0$  (or between  $-\tilde{\chi}_0$  and 0) within a half-period. Therefore, the average value over the half period

$$\langle \tilde{\chi} \rangle = \frac{2}{\lambda_{[001]}} \int_0^{\lambda_{[001]}/2} \tilde{\chi}_0 \sin\left(2\pi \frac{\zeta}{\lambda_{[001]}}\right) d\zeta = \frac{2}{\pi} \tilde{\chi}_0 \quad (35)$$

will be substituted into the left hand side of (34). The length of the half-period  $\lambda_{[001]}/2$  has to be substituted for  $h$ . Finally, taking into account (30) and (31) leads to the following expression for the maximum bending amplitude of a stable crystalline undulator

$$a_s = (0.14 \text{ \AA}) \ln\left(\frac{\lambda_u}{2\sqrt{2} \text{ \AA}}\right). \quad (36)$$

Note that the influence of  $\bar{\chi}$  on the value of  $a_s$  is comparable to the rounding error. The value  $\bar{\chi} = 0.5$  was used in the above calculation.

It was found in experiment [44] that dislocation-free epilayers of much higher thickness and germanium content could be grown than it had been predicted by Matthews-Blakeslee formula (34). The reason for it was the kinetic barrier that had to be overcome before a dislocation could be formed. Therefore, the thickness of a metastable epitaxial layer can exceed the critical value for the stable layer by an order of magnitude or more. In fact, the Matthews-Blakeslee limit reveals itself only after annealing the specimen for about 30 min at 750–900 °C [43].

Several models describing the critical thickness (or, equivalently, the critical germanium content) of a metastable strained layer have been proposed [45, 46, 47]. The formula of People

and Bean<sup>4</sup> [45, 48],

$$\chi_m^2 = \frac{10.9 \text{ \AA}}{h} \ln\left(\frac{h}{4 \text{ \AA}}\right), \quad (37)$$

will be used in the following. It agrees well with the experimental data [44] obtained for a  $\text{Si}_{1-\chi}\text{Ge}_\chi$  layer grown by molecular beam epitaxy at 550 °C.

Repeating the steps that led to formula (36) one obtains the maximum amplitude of a metastable crystalline undulator

$$a_m = \sqrt{(2.4 \cdot 10^{-3} \text{ \AA}) \lambda_u \ln\left(\frac{\lambda_u}{8 \sqrt{2} \text{ \AA}}\right)}. \quad (38)$$

Equations (33), (36) and (38) are summarized in Fig. 4.

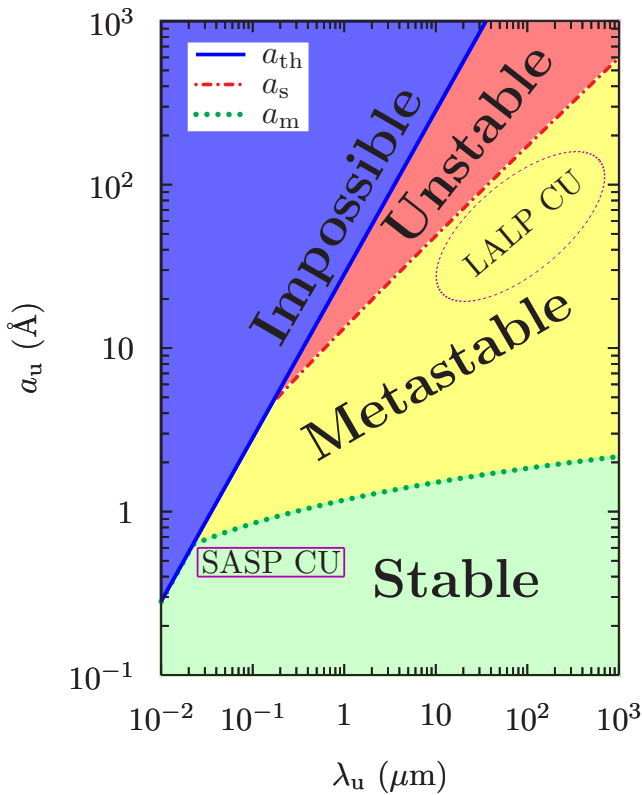


Figure 4: The stability diagram of strained layer crystalline undulator based on graded  $\text{Si}_{1-\chi}\text{Ge}_\chi$  composition vs. the bending period  $\lambda_u$  of the plane (01 $\bar{1}$ ) and the bending amplitude  $a_u$  (see the text for details). The crystalline undulator with a small amplitude and a short period (SASP CU) is predicted to be stable, while that with a large amplitude and a long period (LALP CU) is metastable.

The region  $a_u > a_{th}$  of the diagram is marked as ‘Impossible’. Undulators with such parameters would require the maximum germanium fraction to exceed 100%.

The region  $a_m < a_u < a_{th}$  is called ‘Unstable’. The crystals with the corresponding germanium fraction can be grown, but its crystalline structure will be distorted by misfit dislocations.

<sup>4</sup>The original formula [48] was written in terms of misfit  $f$  related to the germanium fraction  $\chi$  as  $f = 0.0418\chi$ . Therefore it had a different numerical coefficient in the numerator.

As a result, the desired shape of the crystal channel would not be obtained. Therefore, such crystals cannot be used as crystalline undulators.

The ‘Metastable’ region corresponds to  $a_s < a_u < a_m$ ,  $a_{th}$ . Such crystals can be grown and the desired channel shape can be obtained. But the quality of such crystalline undulators may degrade with time. The factors that facilitate the nucleation of dislocations, e.g. heat and ionizing radiation, may accelerate the aging of the strained layer crystal.

Finally, the undulators satisfying  $a_u < a_s$ ,  $a_{th}$  are characterized as ‘Stable’. They are not expected to degrade with time. Moderately high temperatures, not very close to the melting point, are not expected to damage such undulators. Just in opposite, annealing may even improve their quality.

As is seen from the figure, SASP CU, having  $a_u = 0.4\text{--}0.6 \text{ \AA}$  [12], is located in the ‘Stable’ region of the diagram. In contrast, LALP CU, that requires  $a_u \gg d = 1.92 \text{ \AA}$ , can be only metastable.

It has to be stressed that the above statement as well as the whole preceding consideration are valid if the superlattice is macroscopically relaxed, i.e. if there is no external stress acting on it. This is possible if a  $\text{Si}_{1-\chi}\text{Ge}_\chi$  crystal with germanium fraction equal to its average value in the superlattice  $\chi = \bar{\chi}$  is used as a substrate. In this case, the transverse lattice constant  $a_\perp$  of the relaxed superlattice and the substrate are equal. Due to this fact, the substrate does not exert stress on the superlattice. Therefore, the *total* thickness of the superlattice, i.e. the number of undulator periods, is not limited by the instability of the epitaxial layer against misfit dislocations.

In contrast, using a pure silicon crystal as a substrate makes even SASP CU metastable and limits the total thickness of the superlattice. For example, the optimal bending parameters for 855 MeV projectiles,  $\lambda_u = 400 \text{ nm}$  and  $a_u = 0.4 \text{ \AA}$  for electron and  $\lambda_u = 600 \text{ nm}$  and  $a_u = 0.6 \text{ \AA}$  for positron [12], can be obtained at  $\bar{\chi} = 0.017$ . Using equation (37), one finds that the total thickness of a metastable superlattice has to be smaller than 44  $\mu\text{m}$ . In this case, the undulator length (e.g. the superlattice size along the [011] axis) cannot exceed 62  $\mu\text{m}$ .

If one restricts oneself to a thin metastable epitaxial layer, another problem arises if a pure silicon substrate is used.

To let the beam to cross the superlattice without traversing the substrate, a ‘window’ has to be made in the substrate. Otherwise, additional bremsstrahlung and channeling radiation would be produced contributing to the undesirable background. Even if microscopic properties of the superlattice film in the ‘window’ are not influenced by the substrate any more, the size mismatch between the ‘window’ in the pure silicon substrate and the relaxed superlattice may cause a macroscopic deformation of the thin epitaxial layer (figure 5, left). As a result, a variation of the channel entrance angle exceeding 130 mrad at  $\bar{\chi} = 0.017$  may occur. Manufacturing a heterostructure that would be stable against misfit dislocations and the macroscopic deformation simultaneously, if is possible at all, would require a very careful design of the ‘window’ profile and detailed calculations.

No size mismatch and, consequently, no macroscopic deformation of the superlattice takes place if a  $\text{Si}_{1-\bar{\chi}}\text{Ge}_{\bar{\chi}}$  crystal is

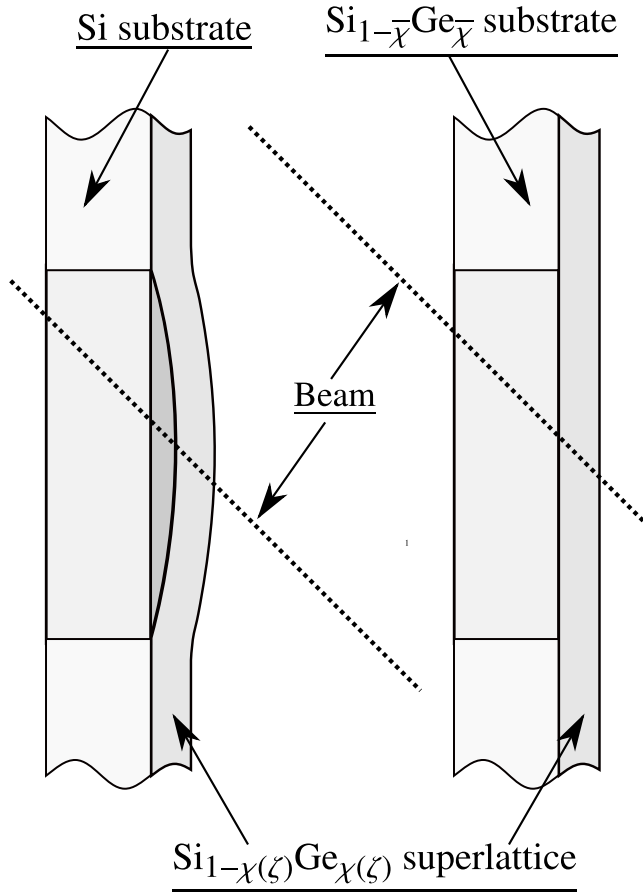


Figure 5: A cross section of the window in the substrate crystal that lets the beam to cross the  $\text{Si}_{1-\chi}\text{Ge}_\chi$  superlattice without crossing the substrate. **Left:** Due to size mismatch between the window in the pure silicon substrate and the relaxed superlattice the latter experiences a macroscopic deformation (depicted with a great exaggeration for illustration purposes). **Right:** No size mismatch and, consequently, no macroscopic deformation are present if a mixed  $\text{Si}_{1-\bar{\chi}}\text{Ge}_{\bar{\chi}}$  crystal with the germanium fraction  $\bar{\chi}$  equal to the average germanium fraction in the heterostructure is used as a substrate.

used as a substrate (figure 5, right). Hence, the  $\text{Si}_{1-\bar{\chi}}\text{Ge}_{\bar{\chi}}$  has a double advantage: it does not put any limit on the thickness of the epitaxial layer and it does not induce macroscopic deformations.

To conclude, a crystalline undulator can be produced by growing a strained layer crystal of a graded  $\text{Si}_{1-\chi}\text{Ge}_\chi$  composition. The germanium content  $\chi$  has to be varied according to Eq. (32) with the variation amplitude  $\tilde{\chi}_0$  calculated from Eq. (30). The obtained crystalline undulators with a small amplitude and a short period (SASP CU) and with a large amplitude and a long period (LALP CU) are predicted to be, respectively, stable and metastable against misfit dislocations, provided that the strained layer crystal is grown on a  $\text{Si}_{1-\bar{\chi}}\text{Ge}_{\bar{\chi}}$  substrate with germanium content equal to its average value  $\bar{\chi}$  in the superlattice. In addition, using the  $\text{Si}_{1-\bar{\chi}}\text{Ge}_{\bar{\chi}}$  prevents macroscopic deformations of the epitaxial layer.

## Acknowledgement

I am grateful to Hartmut Backe for an encouraging discussion.

## References

- [1] J. Lindhard, Influence of crystal lattice on motion of energetic charged particles, *Kongelige Danske Videnskabernes Selskab: Matematisk-Fysiske Meddelelser* 34 (14) (1965) 1–64.
- [2] U. I. Uggerhøj, The interaction of relativistic particles with strong crystalline fields, *Reviews of Modern Physics* 77 (4) (2005) 1131–1171. doi:10.1103/RevModPhys.77.1131.
- [3] V. V. Kaplin, S. V. Plotnikov, S. A. Vorobiev, Radiation of channeled particles in deformed crystals, *Soviet Physics - Technical Physics* 25 (1980) 650–651.
- [4] V. G. Baryshevsky, I. Y. Dubovskaya, A. O. Grubich, Generation of  $\gamma$ -quanta by channeled particles in the presence of a variable external field, *Physics Letters A* 77 (1) (1980) 61–64. doi:10.1016/0375-9601(80)90637-4.
- [5] P. Willmott, *An Introduction to synchrotron radiation: techniques and applications*, John Wiley & Sons, Ltd, 2011. doi:10.1002/9781119970958.
- [6] W. Greiner, A. V. Korol, A. Kostyuk, A. V. Solovyov, Vorrichtung und Verfahren zur Erzeugung elektromagnetischer Strahlung, German Patent DE 10 2010 023 632 (December 15, 2011).
- [7] V. L. Ginzburg, On emission of micro radio waves and their absorption in air, *Izvestiya Akademii Nauk SSSR, Seriya Fizicheskaya* 11 (1947) 165.
- [8] H. Motz, Applications of the radiation from fast electron beams, *Journal of Applied Physics* 22 (5) (1951) 527–535. doi:10.1063/1.1700002.
- [9] H. Motz, W. Thon, R. N. Whitehurst, Experiments on radiation by fast electron beams, *Journal of Applied Physics* 24 (7) (1953) 826–833. doi:10.1063/1.1721389.
- [10] A. V. Korol, A. V. Solov'yov, W. Greiner, Channeling of positrons through periodically bent crystals: on feasibility of crystalline undulator and gamma laser, *International Journal of Modern Physics E: Nuclear Physics* 13 (05) (2004) 867–916. arXiv:physics/0403082, doi:10.1142/S0218301304002557.
- [11] M. A. Kumakhov, On the theory of electromagnetic radiation of charged particles in a crystal, *Physics Letters A* 57 (1) (1976) 17–18. doi:10.1016/0375-9601(76)90438-2.
- [12] A. Kostyuk, Crystalline undulator with a small amplitude and a short period, *Physical Review Letters* 110 (11) (2013) 115503. arXiv:1210.0468, doi:10.1103/PhysRevLett.110.115503.
- [13] A. Kostyuk, Recent progress in the theory of the crystalline undulator, *Nuclear Instruments and Methods in Physics Research Section B: Beam Interactions with Materials and Atoms* 309 (2013) 45–49. arXiv:1303.5034, doi:10.1016/j.nimb.2013.03.012.
- [14] V. G. Baryshevsky, V. V. Tikhomirov, Crystal undulators: from the prediction to the mature simulations, *Nuclear Instruments and Methods in Physics Research Section B: Beam Interactions with Materials and Atoms* 309 (2013) 30–36. doi:10.1016/j.nimb.2013.03.013.
- [15] T. N. Wistisen, K. K. Andersen, S. Yilmaz, et al., Experimental realization of a new type of crystalline undulator, *Physical Review Letters* 112 (25) (2014) 254801. doi:10.1103/PhysRevLett.112.254801.
- [16] U. I. Uggerhøj, T. N. Wistisen, Intense and energetic radiation from crystalline undulators, *Nuclear Instruments and Methods in Physics Research Section B: Beam Interactions with Materials and Atoms* 355 (2015) 35–38. doi:10.1016/j.nimb.2015.02.069.
- [17] S. Bellucci, S. Bini, V. M. Biryukov, et al., Experimental study for the feasibility of a crystalline undulator, *Physical Review Letters* 90 (3) (2003) 034801. arXiv:physics/0208028, doi:10.1103/PhysRevLett.90.034801.
- [18] V. Guidi, A. Antonini, S. Baricordi, et al., Tailoring of silicon crystals for relativistic-particle channeling, *Nuclear Instruments and Methods in Physics Research Section B: Beam Interactions with Materials and Atoms* 234 (1-2) (2005) 40–46. doi:10.1016/j.nimb.2005.01.008.

- [19] E. Bagli, L. Bandiera, V. Bellucci, et al., Experimental evidence of planar channeling in a periodically bent crystal, *The European Physical Journal C - Particles and Fields* 74 (10) (2014) 3114. arXiv:1410.0251, doi:10.1140/epjc/s10052-014-3114-x.
- [20] P. Balling, J. Esberg, K. Kirsebom, et al., Bending diamonds by femtosecond laser ablation, *Nuclear Instruments and Methods in Physics Research Section B: Beam Interactions with Materials and Atoms* 267 (17) (2009) 2952–2957. doi:10.1016/j.nimb.2009.06.109.
- [21] R. O. Avakian, K. T. Avetyan, K. A. Ispirian, E. G. Melikyan, Method for preparation of crystalline undulators, *Nuclear Instruments and Methods in Physics Research Section A: Accelerators, Spectrometers, Detectors and Associated Equipment* 492 (1-2) (2002) 11–13. doi:10.1016/S0168-9002(02)01316-5.
- [22] V. Bellucci, R. Camattari, V. Guidi, et al., Ion implantation for manufacturing bent and periodically bent crystals, *Applied Physics Letters* 107 (6) (2015) 064102. doi:10.1063/1.4928553.
- [23] A. Kostyuk, A. V. Korol, A. V. Solov'yov, W. Greiner, The influence of the structure imperfectness of a crystalline undulator on the emission spectrum, *Nuclear Instruments and Methods in Physics Research Section B: Beam Interactions with Materials and Atoms* 266 (6) (2008) 972–987. arXiv:0710.1363, doi:10.1016/j.nimb.2007.12.107.
- [24] C. Patrignani, et al., Review of Particle Physics, *Chinese Physics C* 40 (10) (2016) 100001. doi:10.1088/1674-1137/40/10/100001.
- [25] U. I. Mikkelsen, E. Uggerhøj, A crystalline undulator based on graded composition strained layers in a superlattice, *Nuclear Instruments and Methods in Physics Research Section B: Beam Interactions with Materials and Atoms* 160 (3) (2000) 435–439. doi:10.1016/S0168-583X(99)00637-0.
- [26] S. C. Jain, J. R. Willis, R. Bullough, A review of theoretical and experimental work on the structure of  $\text{Ge}_x\text{Si}_{1-x}$  strained layers and superlattices, with extensive bibliography, *Advances in Physics* 39 (2) (1990) 127–190. doi:10.1080/00018739000101491.
- [27] S. C. Jain, S. Decoutere, M. Willander, H. E. Maes, SiGe HBTs for application in BiCMOS technology: I. Stability, reliability and material parameters, *Semiconductor Science and Technology* 16 (6) (2001) R51–R65. doi:10.1088/0268-1242/16/6/201.
- [28] D. J. Paul, Si/SiGe heterostructures: from material and physics to devices and circuits, *Semiconductor Science and Technology* 19 (10) (2004) R75–R108. doi:10.1088/0268-1242/19/10/R02.
- [29] M. B. H. Breese, D. G. de Kerckhove, P. J. C. King, P. J. M. Smulders, Direct observation of lattice strain in  $\text{Si}_{1-x}\text{Ge}_x/\text{Si}$  crystals using planar channeling patterns, *Nuclear Instruments and Methods in Physics Research Section B: Beam Interactions with Materials and Atoms* 132 (1) (1997) 177–187. doi:10.1016/S0168-583X(97)00406-0.
- [30] M. B. H. Breese, Beam bending using graded composition strained layers, *Nuclear Instruments and Methods in Physics Research Section B: Beam Interactions with Materials and Atoms* 132 (3) (1997) 540–547. doi:10.1016/S0168-583X(97)00455-2.
- [31] H. Backe, D. Krambrich, W. Lauth, J. Lundsgaard Hansen, U. I. Uggerhøj, X-ray emission from a crystal undulator—Experimental results at channeling of electrons, *Il Nuovo Cimento C* 034 (04) (2011) 157–165. doi:10.1393/ncc/i2011-10938-2.
- [32] H. Backe, D. Krambrich, W. Lauth, et al., Channeling and radiation of electrons in silicon single crystals and  $\text{Si}_{1-x}\text{Ge}_x$  crystalline undulators, *Journal of Physics: Conference Series* 438 (1) (2013) 012017. doi:10.1088/1742-6596/438/1/012017.
- [33] H. Backe, D. Krambrich, W. Lauth, et al., Radiation emission at channeling of electrons in a strained layer undulator crystal, *Nuclear Instruments and Methods in Physics Research Section B: Beam Interactions with Materials and Atoms* 309 (2013) 37–44. doi:10.1016/j.nimb.2013.03.047.
- [34] L. Vegard, Die Konstitution der Mischkristalle und die Raumfüllung der Atome, *Zeitschrift für Physik* 5 (1) (1921) 17–26. doi:10.1007/BF01349680.
- [35] J. P. Dismukes, L. Ekstrom, R. J. Paff, Lattice parameter and density in germanium-silicon alloys, *The Journal of Physical Chemistry* 68 (10) (1964) 3021–3027. doi:10.1021/j100792a049.
- [36] L. D. Landau, E. M. Lifshitz, *Theory of elasticity*, ButterworthHeinemann, 1999.
- [37] W. Krause, A. V. Korol, A. V. Solov'yov, W. Greiner, Photon emission by ultra-relativistic positrons in crystalline undulators: the high-energy regime, *Nuclear Instruments and Methods in Physics Research Section A: Accelerators, Spectrometers, Detectors and Associated Equipment* 483 (1-2) (2002) 455–460. arXiv:physics/0109048, doi:10.1016/S0168-9002(02)00361-3.
- [38] R. Hull (Ed.), *Properties of crystalline silicon*, IET, London, 1999.
- [39] C. Claeys, E. Simoen (Eds.), *Germanium-based technologies: from materials to devices*, Elsevier, Amsterdam, 2007.
- [40] J. H. van der Merwe, Crystal interfaces. Part II. Finite overgrowths, *Journal of Applied Physics* 34 (1) (1963) 123–127. doi:10.1063/1.1729051.
- [41] J. W. Matthews, A. E. Blakeslee, Defects in epitaxial multilayers. I. Misfit dislocations, *Journal of Crystal Growth* 27 (1974) 118–125. doi:10.1016/0022-0248(74)90424-2.
- [42] S. C. Jain, T. J. Gosling, J. R. Willis, D. H. J. Totterdell, R. Bullough, A new study of critical layer thickness, stability and strain relaxation in pseudomorphic  $\text{Ge}_x\text{Si}_{1-x}$  strained epilayers, *Philosophical Magazine, Part A* 65 (5) (1992) 1151–1167. doi:10.1080/01418619208201502.
- [43] D. C. Houghton, The structural stability of uncapped versus buried  $\text{Si}_{1-x}\text{Ge}_x$  strained layers through high temperature processing, *Thin Solid Films* 183 (1-2) (1989) 171–182. doi:10.1016/0040-6090(89)90442-2.
- [44] J. C. Bean, L. C. Feldman, A. T. Fiory, S. Nakahara, I. K. Robinson,  $\text{Ge}_x\text{Si}_{1-x}/\text{Si}$  strained-layer superlattice grown by molecular beam epitaxy, *Journal of Vacuum Science & Technology A: Vacuum, Surfaces, and Films* 2 (2) (1984) 436–440. doi:10.1116/1.572361.
- [45] R. People, J. C. Bean, Calculation of critical layer thickness versus lattice mismatch for  $\text{Ge}_x\text{Si}_{1-x}/\text{Si}$  strained-layer heterostructures, *Applied Physics Letters* 47 (3) (1985) 322–324, erratum: [48]. doi:10.1063/1.96206.
- [46] B. W. Dodson, J. Y. Tsao, Relaxation of strained-layer semiconductor structures via plastic flow, *Applied Physics Letters* 51 (17) (1987) 1325–1327, erratum: [49]. doi:10.1063/1.98667.
- [47] D. C. Houghton, Strain relaxation kinetics in  $\text{Si}_{1-x}\text{Ge}_x/\text{Si}$  heterostructures, *Journal of Applied Physics* 70 (4) (1991) 2136–2151. doi:10.1063/1.349451.
- [48] R. People, J. C. Bean, Erratum: Calculation of critical layer thickness versus lattice mismatch for  $\text{Ge}_x\text{Si}_{1-x}/\text{Si}$  strained-layer heterostructures [Appl. Phys. Lett. 47, 322 (1985)], *Applied Physics Letters* 49 (4) (1986) 229. doi:10.1063/1.97637.
- [49] B. W. Dodson, J. Y. Tsao, Erratum: Relaxation of strained-layer semiconductor structures via plastic flow [Appl. Phys. Lett. 51, 1325 (1987)], *Applied Physics Letters* 52 (10) (1988) 852. doi:10.1063/1.99658.